3.67GHz High-Linearity Low Noise Amplifier With Simple Topology

YINHUA YAO
No.36 Research Institute of CETC
NO. 387, Hongxing Road, Nanhu District,
Jiaxing City, Zhejiang Province
CHINA
yaoyinhua2009@126.com

TONGXIU FAN
No.36 Research Institute of CETC
NO. 387, Hongxing Road, Nanhu District,
Jiaxing City, Zhejiang Province
CHINA
563415726@qq.com

Abstract: This paper describes the design, implementation, and test of a 3.67GHz low noise amplifier (LNA) for intermediate frequency amplifier using pseudomorphic high electron mobility transistor (pHEMT). The LNA circuit is optimized and simulated using Advanced Designed System (ADS). The layout of the amplifier is processed using Protel 99SE. The simulation results show that the gain and noise figure (*NF*) are 13.535dB and 1.47dB with an output 3rd order intercept point (*OIP3*) of 37.441dBm, while input and output voltage standing wave ratios(*VSWRs*) are 1.539 and 1.394, respectively. The tendencies of measured gain, *NF*, and *VSWRs* are in a good agreement with those of simulated ones. The fabricated LNA, with a degraded *NF* below 1.718dB, achieves 13.16dB gain similar to the simulated result. The LNA provides higher than simulations but reasonably acceptable input and output *VSWRs* of 1.539 and 1.710. The measured *OIP3* and output 1dB compression point are better than 33.25dBm and 19.4dBm, respectively.

Key-Words: low noise amplifier, impedance matching, linearity

1 Introduction

Low noise amplifier (LNA) is an essential part of wireless transceivers and as their demands increase so do the requirements for better performance of LNA [1]. In the receiver front-end, the purpose of LNA is to amplify extremely weak input signal from the antenna with minimal noise contribution. In addition, in order not to introduce any distortions, the LNA should also provide a high IP3 (3rd order intercept point). Besides, other specifications also impacting LNA design choices include impedance matchings, stability and gain flatness [2]. In double-conversion receivers, depending on the first intermediate frequency, a specific narrow band LNA is used. A majority of papers on narrow band LNA have been reported, but most of LNAs are perform at 2.4GHz and 5GHz for IEEE 802.11b and 802.11a standard applications [3-6].

In this paper, based on Avago ATF-531P8, an enhanced pHEMT LNA has been designed and implemented for RF receiver front-end with a center frequency of 3.67GHz and bandwidth of 200MHz. ATF-531P8 is ideally suited to meet the needs of wireless communication systems, which demand very high linearity for accurate signal transmission and high transmission power levels with minimum electrical power consumption and component heat generation. To get closer to the practical circuit, the signal transmission lines between two elements are also considered using microstrip lines. Advanced Designed System (ADS) is used to design, simulate, and optimize the circuit, and the layout of LNA is generated using Protel 99SE. Finally, the results are obtained from measurements using Agilent ZVK Vector Network Analyzer, Agilent N8975A Noise Figure Analyzer, Rohde & Schwarz FSP Spectrum Analyzer, and Agilent 8648D Signal Generators. Different from the differential and cascade circuits developed by other authors [3, 7, 8], apart from bias circuits, our proposed LNA topology just consists of input and output DC blocking capacitors acting as matching elements. Such a simple LNA has never been reported, whose objectives such as forward gain dB(S_{21}), low noise figure (*NF*), and good impedance matchings are satisfied simultaneously.

2 Circuit Design

The simulation design is based on a commercial substrate Rogers 4003C with a permittivity 3.38, a loss less than 0.0027 and a thickness 0.508 mm. Fig. 1 shows the topology of the designed amplifier having 50 Ω microstrip lines with a width of 1.12mm regarded as input and output signal transmission lines. According to given datasheet, the LNA is biased at V_{DS}=4V and I_{DS}=135mA with

single supply voltage V_{CC} of +5V. C_2 and C_3 are bypass capacitors, and R_0 and R_1 are voltage-dividing resistors, through which V_{CC} provides an adequate gate voltage. Here, R_0 and R_1 are chosen as 20KΩ and 2.7KΩ. Drain resistor R_2 is used to ensure a proper drain voltage, whose resistance (about 7.5Ω) is obtained through the formula $R_2=(V_{CC}-V_{DS})/I_{DS}$. Inductors L_1 and L_2 are employed to separate RF signals from DC bias conditions. It should be noted that the inductance chosen carelessly will cause self-oscillation of amplifier. C_{in} and C_{out} are input and output DC blocking capacitors, respectively.

In amplifier design, the amplifier has to be kept stable so that it can operate normally. The conditions for unconditional stability of amplifier can be expressed by Rowlett Criteria[9]:

$$K=\frac{1-|S_{11}|^2-|S_{22}|^2+|\Delta|^2}{2|S_{12}S_{21}|}>1 \quad (1)$$

$$|\Delta|=|S_{11}S_{22}-S_{12}S_{21}|<1 \qquad (2)$$

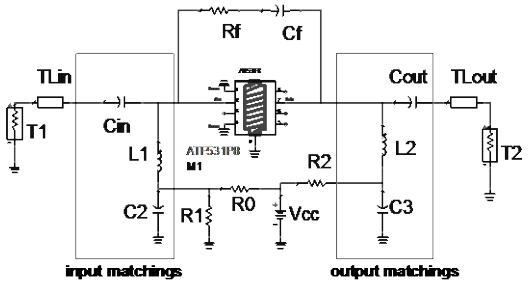

Fig. 1 Topology of the designed amplifier.

In practice, one often examines stable factor K alone without paying attention to the $|\Delta|<1$ condition. During simulation, the instability of amplifier is found at several frequencies below 1GHz. To balance the tradeoff between good matching and unconditional stability in full band (DC-20GHz), one of solutions is to add a shunt negative feedback path [10]. As well known to us, negative feedback can not only widen the bandwidth in wideband amplifier design, but also enhance the stability of amplifier [11]. Alternatively, we can add a series or shunt resistor in input or output port, but the additional resistor will deteriorate the noise figure seriously.

Fig. 2 shows the characteristic impedances, typical S parameters, and noise figure of pHEMT biased at V_{DS}=4V and I_{DS}=135mA. The input and output impedances are Z_1=7.427+j10.325=r_1+jx_1 Ω and Z_2=20.558+j4.789=r_2+jx_2 Ω. Noise figure (1.191dB) at 3.67GHz is good, but the forward gain dB(S_{21}) is quite poor only, 8.861dB, and input and output ports mismatch seriously. Therefore, additional input and output matching circuits, which aim at matching Z_{in} and Z_{out} to 50Ω source impedance (R_S) and load impedance (R_L), are necessary to improve the poor performances. Since the input and output of pHEMT device are primarily inductive, we can terminate the input and output with capacitors. The designed matching circuits are typical L-type networks,

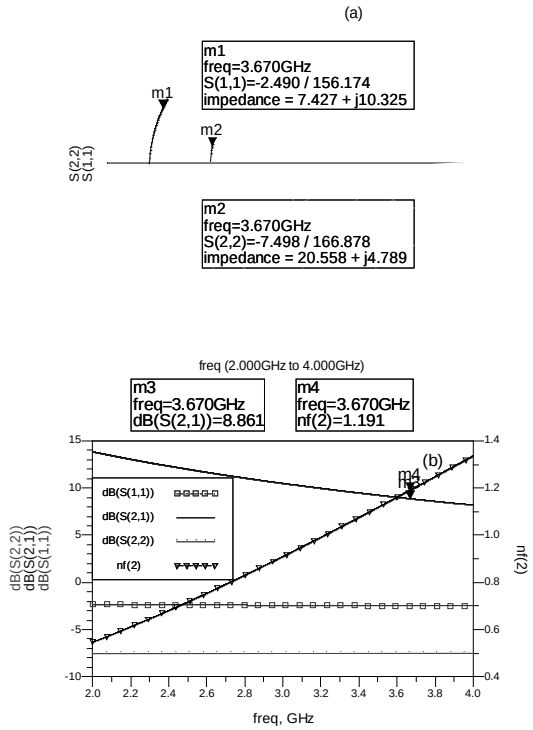

Fig. 2 Input and output impedances of ATF-531P8.

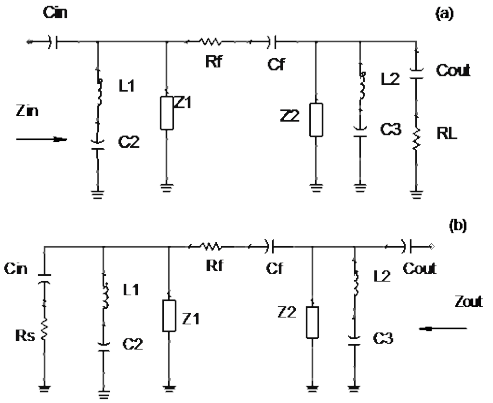

Fig.3 (a) Input and (b) output impedances of LNA.

where, some elements including L_1, C_2, L_3, and C_3 also function in the bias circuit stated above. After matchings, the input and output impedances of amplifier are transformed into Z_{in} and Z_{out}, shown in Fig. 3. Bypass capacitors C_2 and C_3 and feedback capacitors C_f of 1000pF can be regarded as short circuits at f_0=3.67GHz. Thus, Z_{in} and Z_{out} are expressed as:

$$Z_{in} = \frac{1}{j\omega C_{in}} + (j\omega L_1 // Z_1) // [R_f + Z_2 // j\omega L_2 // (R_L + \frac{1}{j\omega C_{out}})] \quad (3)$$

$$Z_{out} = \frac{1}{j\omega C_{out}} + (j\omega L_2 // Z_2) // [R_f + Z_1 // j\omega L_1 // (R_s + \frac{1}{j\omega Cin})] \quad (4)$$

From the formula Gain[dB]=20log|S_{21}| (dB), in order to obtain a gain above 10dB, log| S_{21}| has to be larger than 0.5dB and |S_{21}| higher than 3.16. The S_{21} parameter of an amplifier with negative feedback is approximately written as [11]:

$$S_{21} = (Z_0 - R_f) / Z_0 \quad (5)$$

Where, Z_0 is the characteristic impedance, 50Ω. Consequently, R_f is determined to be 208Ω at least, which leads to the validity of expressions (6) and (7).

$$(j\omega L_1 // Z_1) << [R_f + Z_2 // j\omega L_2 // (R_L + \frac{1}{j\omega C_{out}})] \quad (6)$$

$$(j\omega L_2 // Z_2) << [R_f + Z_1 // j\omega L_1 // (R_s + \frac{1}{j\omega C_{in}})] \quad (7)$$

Therefore, Z_{in} and Z_{out} can be further simplified as:

$$Z_{in} = \frac{1}{j\omega C_{in}} + (j\omega L_1 // Z_1) \quad (8)$$

$$Z_{out} = \frac{1}{j\omega C_{out}} + (j\omega L_2 // Z_2) \quad (9)$$

These indicate that the introduced feedback circuit has little effect on the input and output impedances when R_f is further larger than the impedances of pHEMT. By changing these values of lumped elements properly, $|z_{in}| = R_S$ or $|z_{out}| = R_L$ can be satisfied, and the maximum power matching or optimization noise matching is obtained. However, they can not be satisfied simultaneously, and therefore, we have to balance the tradeoff between high gain and low *NF*. For achieve satisfied and better gain, *VSWRs*, and *NF*, these values are optimized using ADS. The resulting input and output impedances are graphically shown in Fig. 4. From Fig. 4, the magnitudes of Z_{in} and Z_{out} are 62.769Ω and 36.2Ω, respectively, while good reflection coefficients (S_{11} and S_{22}) are seen, -13.457dB and -15.673dB. These results confirm the good impedance matchings.

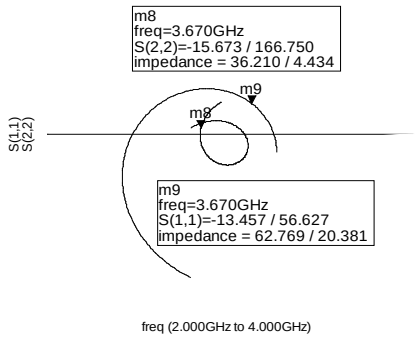

Fig. 4 Resulting input and output impedances.

3 Simulation Results

The *K* plot as illustrated in Fig. 5(a) demonstrates unconditional stability of the LNA. As stated above, it is mainly attributed to the introduction of negative feedback path. Fig. 5(b) depicts the input and output *VSWRs* of 1.539 and 1.394 at 3.67GHz with little change in the frequency range of 3.57-3.77GHz. The LNA achieves not only good matchings, but also reasonably acceptable noise and gain performance. Seen from Fig. 4(c), *NF* is near 1.470dB in the whole frequency range, and gain varies between 13.329dB and 13.698dB with 13.53dB at 3.67GHz. In additions, Fig. 4(d) displays that an *OIP3* of 37.441dBm is achieved.

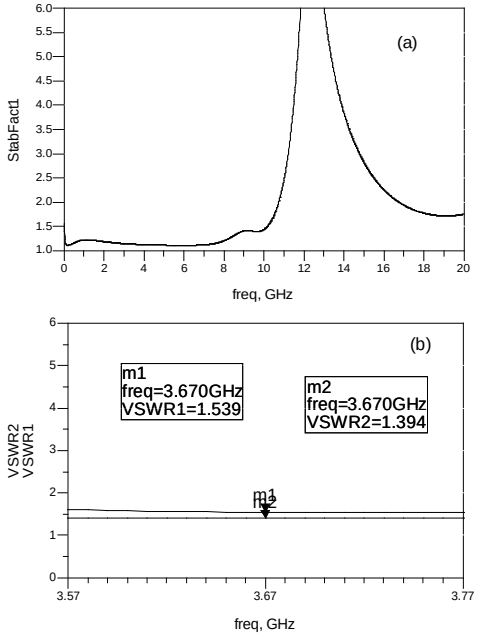

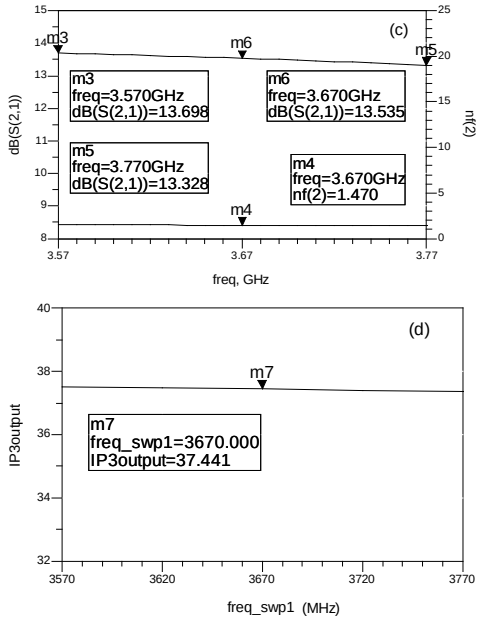

Fig. 5 Simulation results for (a) stability factor *K*, (b) *VSWR1* and *VSWR2*, (c) *NF* and gain (d) *OIP3*.

4 Fabrication and Test

In the LNA design, the final step is the layout process, which allows designers to have their circuits manufactured. The layout is generated using Software Protel 99SE, and its area is about $22.12\times11.64mm^2$. Fig. 6 displays the photograph of the assembled LNA.

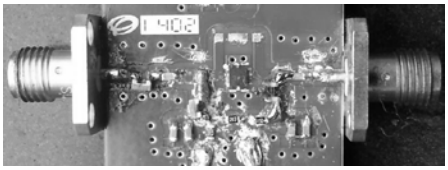

Fig. 6 Photograph of fabricated LNA

The gain, input reflection coefficient (S_{11}), and *VSWRs* are measured with Agilent ZVK Vector Network Analyzer. In the process of measuring and tuning, it is noted that the LNA can work normally without feedback path, as a result of which, the feedback network is disconnected. The following good performances are obtained and illustrated in Fig. 7. In the desired operating frequency the gain with little variation is 13.16dB at centre frequency similar to that simulated value and input reflection coefficient (S_{11}) is below -13dB. *VSWR1* and *VSWR2* are 1.539 and 1.710, respectively, whose curves are similar to the simulated those.

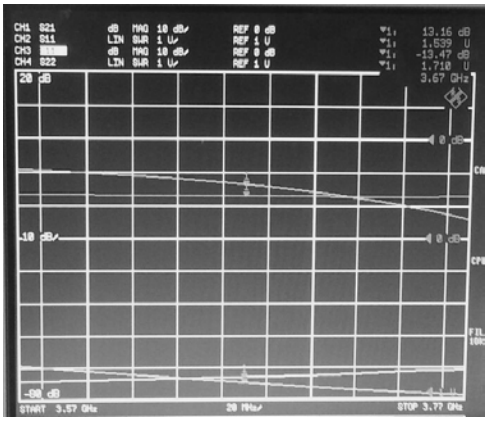

Fig. 7 Measured results for gain and *VSWRs.*

The noise figure is investigated using Agilent N8975A Noise Figure Analyzer. From Fig. 8, *NF* is less than 2dB at the frequencies of interest, and 1.718dB at 3.67GHz. The IP3 performance is measured with Rohde & Schwarz FSP Spectrum Analyzer and Agilent 8648D Signal Generators. Continuous wave signals are applied to characterize the three order intermodulation (IM_3) performance, as shown in Fig. 9. The carrier frequencies of two signal sources are 3.67GHz and 3.671GHz, respectively. It can be seen that the fundamental output power is 7.15dBm, and the output power of IM_3 is -45.03dBm at 3.672GHz. Thus, the IM_3 distortion (IMD_3) is about -52.2dBc, and OIP3 is 33.25dBm. When input power increases to 13dBm, the tested output 1dB compression point (P_{1dB}) is 19.4dBm. Except for the gain, the measured *VSWRs*, *NF*, and OIP3 are inferior to those simulated values. In our opinions, the difference between measured and simulated results is attributed to board losses and parasitic parameters of pHEMT. Compared with the data from other LNAs listed in Ref [5, 6], our results show a higher IP3. Moreover, the proposed topology of LNA is quite simple.

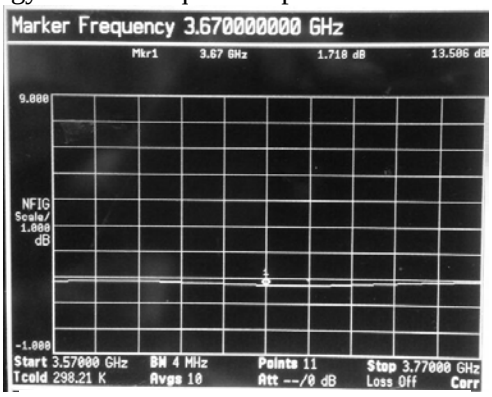

Fig. 8 Measured result for noise figure

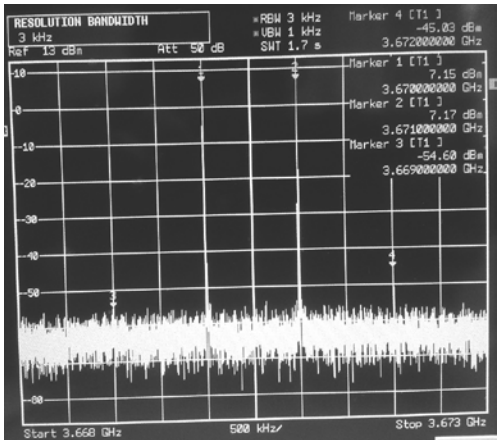

Fig. 9 Measured result for IP3 performance.

5 Conclusion

A 3.57-3.77GHz low noise amplifier with a simple topology has been designed, fabricated, and tested, which is just composed of input and output matching capacitors and bias circuit. The proposed LNA circuit involves L-type matching networks, where some elements are parts of the DC bias circuit. After matching, the performances of amplifier are improved vastly. The simulated LNA exhibits a gain of 13.535dB and a noise figure of 1.47dB with an output 3rd order intercept point of 37.441dBm. The input and output voltage standing wave ratios are 1.539 and 1.394, respectively. In contrast, degraded measured properties are thought to be board loss and parasitic parameters of packing pHEMT. The fabricated LNA provides *VSWR1* of 1.539, *VSWR2* of 1.710, and gain of 13.33dB at 3.67GHz with little change within the required bandwidth. The *OIP3* and P_{1dB} are 33.25dBm and 19.4dBm respectively, while the noise figure is 1.718 dB. Such LNA can be used as first intermediate frequency amplifier in double-conversion receivers and other wireless communication systems.

References:

[1] P. Y. Chang, S. H. Su, S. S. H. Hsu, W. H. Cho, and J. D. Jin, An ultra-low-power transformer-feedback 60 GHz low-noise amplifier in 90 nm CMOS. *IEEE Microwave and Wireless Component Letters*, vol. 22, No. 4, 2012, pp. 197-199.

[2] M. Kraemer, D. Dragomirescu, and R. Plana, A low-power high-gain LNA for the 60 GHz band in a 65 nm CMOS technology. *Proceeding of Asia Pacific Microwave Conference*, Singapore, 2009, pp.1156-1159.

[3] M. Sumathi and S. Malarvizhi, Performance Comparison of RF CMOS Low Noise Amplifiers in 0.18-µm technology scale. *International Journal of VLSI design & Communication Systems (VLSICS)*, vol. 2, 2011, pp.45-54.

[4] Y. Jaehyuk and P. Changkun, 5-Ghz low noise amplifier with ESD protection method using transformer. *Microwave and Optical Technology Letters*, vol. 56, No. 3, 2014, pp. 684–689.

[5] M. J. Zavarei, E. Kargaran, Nabovati, and Hooman, New linearization method for low voltage, low power folded cascode LNAs. *Proceeding of 2012 IEEE 55th International Midwest Symposium on Circuits and Systems (MWSCAS)*, Boise, America, 2012, pp. 738-741.

[6] B. M. Liu, C. H. Wang, M. L. Ma, and S. Q. Guo, An ultra-low-voltage and ultra-low-power 2.4GHz LNA design. *Radioengineering*, vol. 18, No. 4, 2009, pp.527-531.

[7] A. B. Ibrahim, A. R. Othman, M. N. Husain, and M. S. Johal, Low noise, high gain LNA at 5.8GHz with cascode and cascaded techniques using T-matching network for wireless applications. *International Journal of Information and Electronics Engineering*, vol. 1, No. 2, 2011, pp.146-149.

[8] M. C. Praveen, V. V. Venkatesan, J. Raja, and R. Srinivasan, Active inductor based differential low noise amplifier for ultra wide band applications. *Proceeding of 2012 International Conference on Recent Trends In Information Technology (ICRTIT)*, Chennai, India, 2012, pp. 19-21.

[9] R. Ludwing and G. Bogdanov, *RF Circuit Design Theory and Application*, 2nd ed. Beijing: Publishing house of electronics industry, 2008, pp. 476.

[10] H. Sahoolizadeh, A. M. Kordalivand, and Z. Heidari, Design and simulation of low noise amplifier circuit for 5 GHz to 6 GHz. *World Academy of Science, Engineering and Technology*, vol. 51, 2009, pp.99-101.

[11] Y. H. Yao and T. X. Fan, Design of wideband high gain and low noise amplifiers. *International Journal of Information and Electronics Engineering*. Vol. 4, No. 6, 2014, pp. 456-450.